Kinetic Studies on the Interaction between a Ribosomal Complex Active in Peptide Bond Formation and the Macrolide Antibiotics Tylosin and Erythromycin

George P. Dinos* and Dimitrios L. Kalpaxis

Laboratory of Biochemistry, School of Medicine, University of Patras, 26500 Patras, Greece

Received April 11, 2000; Revised Manuscript Received July 11, 2000

ABSTRACT: The inhibition of peptide bond formation by tylosin, a 16-membered ring macrolide, was studied in a model system derived from *Escherichia coli*. In this cell-free system, a peptide bond is formed between puromycin (acceptor substrate) and AcPhe-tRNA (donor substrate) bound at the P-site of poly(U)-programmed ribosomes. It is shown that tylosin inhibits puromycin reaction as a slow-binding, slowly reversible inhibitor. Detailed kinetic analysis reveals that tylosin (I) reacts rapidly with complex C, i.e., the AcPhe-tRNA·poly(U)·70S ribosome complex, to form the encounter complex CI, which then undergoes a slow isomerization and is converted to a tight complex, C*I, inactive toward puromycin. These events are described by the scheme C + I $\rightleftarrows$ (K_i) CI $\leftrightharpoons$ (k_4, k_5) C*I. The K_i, k_4, and k_5 values are equal to 3 μM, 1.5 min^{-1}, and 2.5 × 10^{-3} min^{-1}, respectively. The extremely low value of k_5 implies that the inactivation of complex C by tylosin is almost irreversible. The irreversibility of the tylosin effect on peptide bond formation is significant for the interpretation of this antibiotic's therapeutic properties; it also renders the tylosin reaction a useful tool in the study of other macrolides failing to inhibit the puromycin reaction but competing with tylosin for common binding sites on the ribosome. Thus, the tylosin reaction, in conjunction with the puromycin reaction, was applied to investigate the erythromycin mode of action. It is shown that erythromycin (Er), like tylosin, interacts with complex C according to the kinetic scheme C + Er $\rightleftarrows$ (K_{er}) CEr $\rightleftarrows$ (k_6, k_7) C*Er and forms a tight complex, C*Er, which remains active toward puromycin. The determination of K_{er}, k_6, and k_7 enables us to classify erythromycin as a slow-binding ligand of ribosomes.

Macrolide antibiotics, a rather large group of naturally occurring inhibitors of protein synthesis, contain a large lactone ring substituted with one or more sugar residues, some of them amino sugars (*1*). They can be roughly divided into two main groups which are structurally and functionally homogeneous and which are typically represented by erythromycin and spiramycin, respectively (*2*, *3*). The erythromycin group includes compounds with a 14-membered lactone ring glycosylated in two positions by different monosaccharides, while the spiramycin group consists of compounds with a 16-membered lactone ring usually glycosylated at a single position by a disaccharide. The larger ring macrolides, such as spiramycin and tylosin, act at the level of the large ribosomal subunit and behave as typical inhibitors of peptidyltransferase. They inhibit most of the protein synthesis assay systems, possibly by destabilizing the P-site-bound peptidyl-tRNA or by blocking the exit channel for the growing peptide chain, but they are unable to block translation when the nascent peptide chain has reached a certain length (*1*, *3*, *4*). On the other hand, erythromycin exhibits a marginal inhibitory effect, unless donor substrates with a peptidyl moiety of specific length and nature are employed in these assays (*5*). Nevertheless, numerous studies in the literature are referred to the erythromycin interaction either with vacant ribosomes or with ribosomal subparticles (*1*, *5*−*10*). Although the precise mechanism for translation inhibition by erythromycin is not yet understood, it seems that erythromycin affects the interaction of peptidyl-tRNA with the P-site (*11*−*13*) and prevents the formation of 50S ribosomal subunit in growing bacterial cells (*14*). Despite the observed divergences in the mode of action among the members of the above-mentioned groups, all macrolides seem to compete for similar or overlapping binding sites on the large ribosomal subunit. Thus, cross-resistance to different macrolides is associated with mutations situated in the peptidyltransferase domain (domain V of 23S rRNA) and in domain II, as well as in ribosomal proteins (*3*, *15*). Dissociated resistance to certain macrolides has been also reported (*2*). These observations have been confirmed by footprinting analysis (*4*, *7*, *16*), as well as by reconstitution and affinity labeling experiments (*3*).

On the assumption that the interaction of macrolides (I) with ribosomes (R) could be represented by a fast equilibrated equation, R + I (K_i) $\rightleftarrows$ RI, their potency has been expressed on the basis of K_i alone (*17*, and references therein). Despite this seemingly satisfactory modeling, it has been demonstrated from a previous kinetic study in our laboratory (*18*) that one of these macrolides, spiramycin, does not act simply by binding but that binding induces a conformational change in the ribosome, thereby interfering with peptidyltransferase activity. Furthermore, it has been recently reported (*9*) that two different types of interactions between macrolides and *Escherichia coli* ribosomes exist: a strong interaction (K_d = 10^{-7}−10^{-9} M) classically measured by binding assays and a weak interaction (K_d = 10^{-3}−10^{-5} M) detected by transferred nuclear Overhauser effect

* To whom correspondence should be addressed: tel, 3061-996259; fax, 3061-997690; e-mail, geodinos@med.upatras.gr.

10.1021/bi000811f CCC: $19.00
Published on Web 08/31/2000

(TRNOE)[1] studies. In view of the above observations, we thought it was interesting to examine another member of the macrolide family, tylosin. A better understanding of peptidyltransferase response to macrolide attack will have an impact not only in basic research but also in clinical applications.

The data presented here demonstrate that tylosin inhibits peptidyltransferase activity in a two-step mechanism. The values of the rate constants pertaining to the interaction of tylosin with the ternary complex AcPhe-tRNA·poly(U)·70S ribosome are very low, allowing the classification of tylosin as a slow-binding, slowly reversible inhibitor. Such properties render tylosin a useful tool to study the interaction of ribosomes with other antibiotics failing to inhibit the puromycin reaction. An application of this strategy to the investigation of the erythromycin mode of action is presented.

EXPERIMENTAL PROCEDURES

Materials. L-Phenylalanine, poly(U), GTP (disodium salt), ATP (disodium salt), puromycin dihydrochloride, tRNA from *E. coli* strain W, tylosin, and erythromycin were purchased from Sigma Chemical Co. L-Phenyl-[2,3,4,5,6-^{3}H]alanine was purchased from Amersham Life Science. Cellulose nitrate filters (type HA, 24 mm diameter, 0.45 μm pore size) were from Millipore Corp. Scintillation cocktail safefluor S was purchased from Lumac LSC.

Biochemical Preparations. Salt-washed ribosomes (0.5 M NH_4Cl) and translation factors partially purified were obtained from *E. coli* B cells as reported previously (*19*). Crude Ac[^{3}H]Phe-tRNA (2000 cpm/pmol) and complex C, i.e., the Ac[^{3}H]Phe-tRNA·poly(U)·70S ribosome complex, were prepared as described elsewhere (*18*, *19*). The formed complex C was adsorbed on cellulose nitrate filters and washed with three 4-mL portions of cold buffer (100 mM Tris-HCl, pH 7.2/50 mM KCl/10 mM $MgCl_2$/6 mM 2-mercaptoethanol). Alternatively, complex C was desorbed into a solution containing the detergent Zwittergent 3-12, (ZW extract) according to a method described previously (*20*).

Puromycin Reaction. The reaction between complex C and an excess of puromycin was carried out at 10 mM Mg^{2+} and 100 mM NH_4^+, as described previously (*20*). Briefly, complex C reacted with an excess of puromycin in the presence or in the absence of macrolides, and the progress of the reaction was analyzed over a wide range of puromycin and macrolide concentrations. When desired, the reaction was terminated by addition of an equal volume of 1 M NaOH. The product, AcPhe-puromycin, was extracted in ethyl acetate, and the radioactivity was measured in a liquid scintillation spectrometer. In the kinetic analysis, the product is expressed as a percentage of the isolated complex C on the filter [$100(P/C_0)$]. Controls without poly(U) were included in each experiment, and the values obtained were subtracted.

Inactivation of Complex by Tylosin in the Absence of Puromycin. Complex C adsorbed on a cellulose nitrate filter reacted with various concentrations of tylosin in a 2 mL buffer solution (100 mM Tris-HCl, pH 7.2/100 mM NH_4Cl/10 mM Mg^{2+} (acetate)/6 mM 2-mercaptoethanol). The reaction was allowed to proceed at 25 °C for the desired time intervals and was stopped by immersing the filter in 15 mL of cold buffer. The remaining active complex C, after the cellulose nitrate filter was washed to remove traces of tylosin not specifically bound, was determined by titration with puromycin (2 mM, 2 min at 25 °C). The inactivation of complex C by tylosin was also examined in the presence of erythromycin. In another series of experiments, complex C was first exposed to erythromycin for specified periods of time (preincubation step), and subsequently tylosin was added and allowed to react for the indicated time intervals. The inactivation of complex C was monitored as mentioned above.

When complex C was desorbed in solution, the inactivation took place in 1 mL of buffer solution containing tylosin in the appropriate concentration, and the reaction was stopped by dilution with cold buffer (*18*). Following filtration and wash with the same buffer, the remaining active complex C was titrated by puromycin as above.

Calculation of the Rate Constant Values and Statistical Analysis. The values of the rate constants were obtained by linear regression fitting of kinetic data to eqs 1−4 and A5−A10, using the Microcal Origin 40 program (Microcal Software, Inc.). All data presented in the figures denote the mean values obtained from four independently performed experiments. The standard error of the means was calculated according to Daniel (*21*).

Scheme 1

$$C + S \underset{}{\overset{K_s}{\rightleftharpoons}} CS \xrightarrow{k_3} C' + P$$

RESULTS

Inhibition of Peptide Bond Formation by Tylosin. The reaction between complex C and excess puromycin (S) proceeds as an irreversible pseudo-first-order reaction according to the kinetic Scheme 1. C′ is a modified species of complex C not participating in re-forming complex C, and P is the product (AcPhe-puromycin). The relationship

$$\ln\frac{C_0}{C_0 - P} = k_{obs}t \qquad (1)$$

holds; C_0 is the reactive complex C at zero time, and k_{obs} is the apparent rate constant of product formation. k_{obs} is related to the puromycin concentration by the equation:

$$k_{obs} = \frac{k_3[S]}{K_s + [S]} \qquad (2)$$

which allows the determination of k_3 and K_s values (*22*). These values are equal to 2 min^{-1} and 4×10^{-4} M, respectively. In conformity to eq 1, the progress curve of the puromycin reaction is a straight line at 4×10^{-4} M puromycin (Figure 1A, upper line). However, in the presence of tylosin the rate of product formation is slower, and each time plot reaches a plateau which progressively bends down with increasing concentrations of tylosin. This inhibition pattern suggests that tylosin inactivates complex C rather irreversibly. It is also apparent that the initial slope of

[1] Abbreviations: complex C, the Ac-[^{3}H]Phe-tRNA·poly(U)·70S ribosome complex that bears Ac-[^{3}H]Phe-tRNA bound at the ribosomal P site; ZW, Zwittergent, the detergent *N*-dodecyl-*N*,*N*-dimethyl-3-ammonium-1-propanesulfonate; TRNOE, the transferred nuclear Overhauser effect.

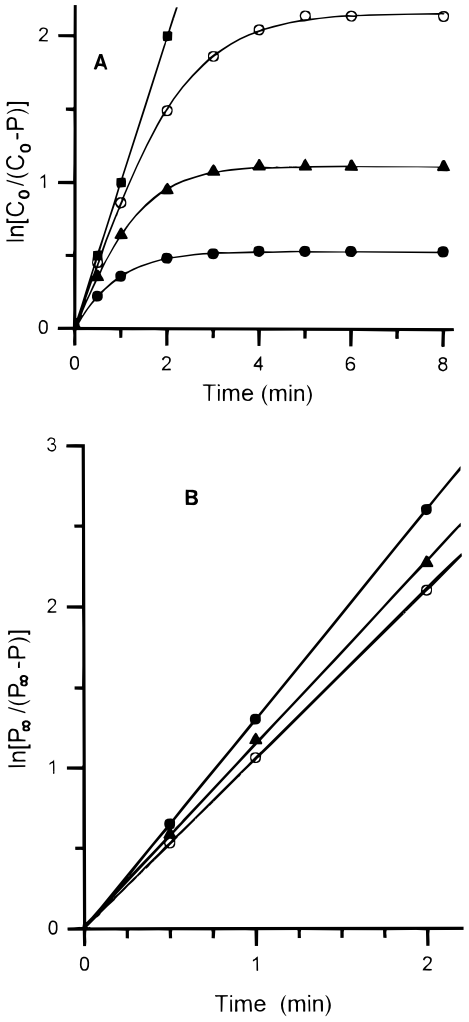

FIGURE 1: (A) First-order time plots for AcPhe-puromycin formation in the presence or in the absence of tylosin. Complex C adsorbed on a cellulose nitrate filter reacted with (■) 4×10^{-4} M puromycin in the absence or in the presence of tylosin at (○) 0.6×10^{-6} M, (▲) 2×10^{-6} M, and (●) 6×10^{-6} M. (B) Replot of the data of (A) in the form of $\ln[P_\infty/(P_\infty - P)]$ versus time. P_∞ represents the product at infinite time and is practically estimated from the maximal level of the *A* plots.

progress curves varies as a function of the inhibitor concentration, supporting inactivation of complex C by a two-step mechanism (*23*). Whereas in most catalyzed reactions the enzyme is regenerated after each catalytic event, in the puromycin reaction the enzyme (complex C) is consumed, and there is no enzyme turnover. Kinetic analysis of the puromycin reaction in the presence of an irreversible inhibitor has been presented previously (*18*, *24*). Taking into account this analysis, the data presented in Figure 1A were replotted in the form of $\ln[P_\infty/(P_\infty - P)]$ versus time (Figure 1B), where P_∞ is the product at infinite time. The linearity of plots illustrated in Figure 1B indicates that the data obey the equation

$$\ln\frac{P_\infty}{P_\infty - P} = At \qquad (3)$$

which represents the integrated kinetic law of complex C inactivation via two parallel and irreversible reactions, the puromycin reaction and the tylosin reaction. The parameter

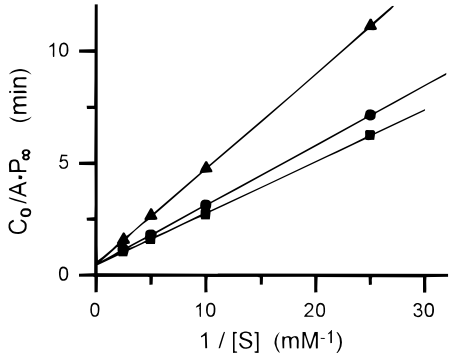

FIGURE 2: Dependence of C_0/AP_∞ on the reciprocal of puromycin concentration. Experiments were performed at (■) 0.4×10^{-6} M, (●) 1×10^{-6} M, and (▲) 4×10^{-6} M tylosin. The parameter *A* expresses the apparent rate constant for complex C inactivation by both tylosin and puromycin.

Scheme 2

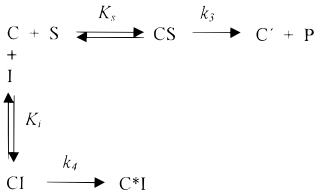

A expresses the apparent rate constant for the inactivation of complex C (*24*), and its value at each concentration of puromycin and tylosin can be obtained from the slope of straight lines, like those depicted in Figure 1B. At each concentration of puromycin, the replot of the *A* value versus tylosin concentration (not shown) deviates from linearity and is characterized by a clear hyperbolic shape suggesting that a two-step mechanism of inhibition may exist. Moreover, the plot of C_0/AP_∞ versus 1/[S] is linear at each concentration of tylosin. In this case, the intercept on the vertical axis is constant, while the slope varies as a function of tylosin concentration (Figure 2). According to previous studies on the inhibition of enzymes consumed during the reaction they catalyze (*18*, *24*), such a behavior corresponds specifically to the competitive mode of action. Consequently, a kinetic scheme that could adequately explain the above-mentioned results is Scheme 2.

Inactivation of Complex C by Tylosin. Additional evidence in support of the mechanism of tylosin interaction with complex C was sought by reacting complex C with tylosin in the absence of puromycin. In these experiments, the inactivation of complex C was examined by exposing the ribosomal complex to various tylosin concentrations for several time intervals and titrating the remaining catalytic activity by puromycin. Inactivation plots at several concentrations of tylosin are shown in Figure 3A. All of them are represented by descending straight lines, intersecting the vertical axis at a common point. This pattern leads to the conclusion that the inactivation of complex C follows pseudo-first-order kinetics. From the slope of each straight line, we can estimate a pseudo-first-order rate constant of inactivation (k_{in}). The k_{in} values, if plotted against the concentration of tylosin, give a rectangular hyperbolic curve (not shown), further supporting the two-step mechanism of inactivation (*25*). As expected, the double-reciprocal plot is given by a straight line intercepting the vertical axis at a point above 0 (Figure 3B). Assuming that the kinetic scheme

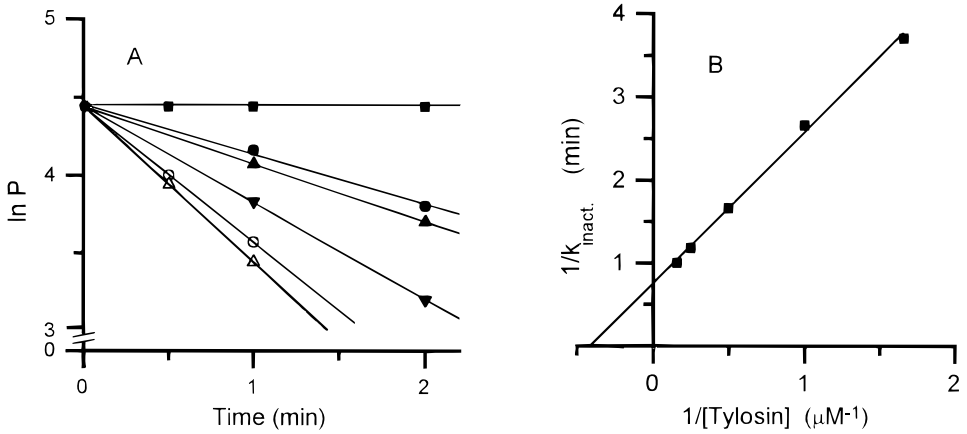

FIGURE 3: (A) First-order time plots for the inactivation of complex C by tylosin. Complex C adsorbed on a cellulose nitrate filter was incubated with tylosin at (△) 6×10^{-6} M, (○) 4×10^{-6} M, (▼) 2×10^{-6} M, (▲) 1×10^{-6} M, and (●) 0.4×10^{-6} M at 25 °C for the indicated time intervals. The excess of tylosin was then removed, and the remaining active complex C was titrated with 2 mM puromycin. Experiments of complex C titration in the absence of tylosin (■) were also performed. (B) Double-reciprocal plot ($1/k_{in}$ versus 1/[I]) for the inactivation of complex C by tylosin. The k_{in} values were estimated from the slope of the *A* plots.

of complex C inactivation by tylosin is correct, the relationship

$$k_{in} = \frac{k_4[I]}{K_i + [I]} \quad (4)$$

holds (*25*), and the values of K_i and k_4 can be determined from the double-reciprocal plot of eq 4 (Figure 3B). These values were found to be equal to 3 μM and 1.5 min^{-1}, respectively.

Reversibility of Complex C Inactivation by Tylosin. When k_{off} assumes a very low value, the binding of an inhibitor to the enzyme becomes very strong. In such a case, it may be difficult to distinguish irreversible from slowly reversible inhibition. With tight-binding inhibitors, which allow separation of E*I from free inhibitor, the reversibility of the inactivation step can be inferred from the recovery of enzymatic activity after dilution of the E*I complex into a large volume of buffer containing near-saturating substrate. Such a treatment reduces the rate of reassociation of inhibitor to the enzyme and permits the measurement of the enzyme regeneration rate from the inactive E*I complex (*26*). A very slow recovery of activity is actually observed when C*I is treated as above (Figure 4). A steady state for the reaction is reached after 2 min, with a k_{off} rate constant (k_5) equal to $(2.5 \pm 0.25) \times 10^{-3}$ min^{-1}.

Inactivation of Complex C by Tylosin in the Presence of Erythromycin. Earlier works have demonstrated that erythromycin does not inhibit in vitro translation systems, in which AcPhe-tRNA is used as a donor substrate (*5*). We also found that erythromycin fails to inhibit the puromycin reaction with complex C. This renders the study of erythromycin interactions with complex C impossible, if what we examine is its effects simply on peptide bond formation. However, erythromycin competes with tylosin for common binding sites on the ribosome (*5*). This fact was exploited as follows: the experiments of complex C inactivation by tylosin were repeated in the presence of increasing concentrations of erythromycin, and the subsequent changes in the rate constant of inactivation were monitored. As shown in Figure 5A, when a mixture of tylosin with erythromycin is used in place of tylosin alone, a decrease in the apparent rate constant of

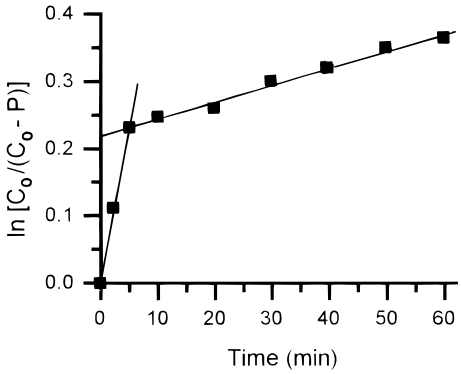

FIGURE 4: Regeneration of complex C from the tylosin complex C*I. Complex C adsorbed on a cellulose nitrate filter was preincubated with 20 μM tylosin for 5 min at 25 °C. The excess of tylosin was removed by washing, and the filter was immersed into 5 mL of reaction buffer containing 2 mM puromycin for several time intervals. The rate constant of the enzymatic activity regain was measured from the slope of the line at the steady state.

inactivation occurs. At high concentrations of erythromycin the protection of complex C against tylosin is complete (Figure 5A, upper line). According to eq A9 (see Appendix), the slope of the plots, like those presented in Figure 5A, gives the apparent rate constant of inactivation (*F*), which depends on the concentration of both erythromycin (Er) and tylosin (I). On the basis of these results and taking into account that erythromycin interacts with *E. coli* ribosomes by a two-step mechanism (*9*), we postulate Scheme 3 for the competition of tylosin reaction by erythromycin. As predicted by eq A7, at each concentration of tylosin the plot *1/F* versus erythromycin concentration is a straight line. Figure 5B shows such a plot obtained at 4 μM tylosin and varying erythromycin concentrations. From the slope of this plot (slope $= K_i/k_4K_{er}[I]$) a K_{er} value equal to 3.9×10^{-7} M can be estimated. K_{er} values measured at different concentrations of tylosin (I) according to equation A8 do not vary by more than 10%.

When preincubation of complex C with erythromycin precedes the addition of tylosin, a further decrease in the apparent rate constant of inactivation occurs. This effect (preincubation effect) supports the notion that at least one of the sequential steps of complex C interaction with

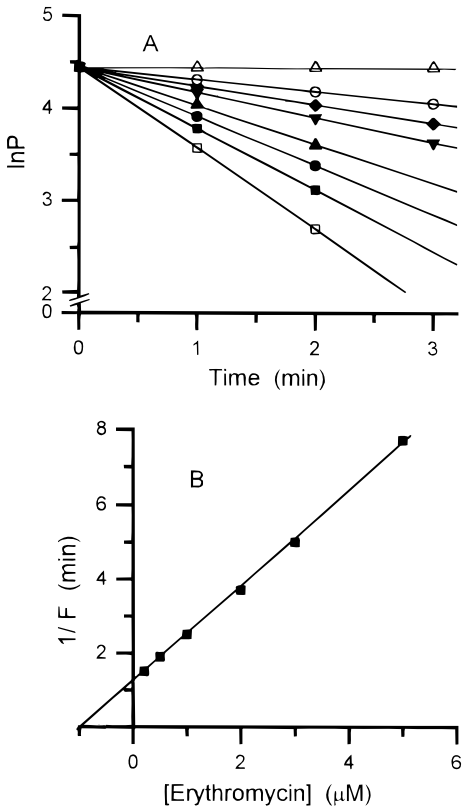

FIGURE 5: Effect of erythromycin on the inactivation of complex C by tylosin. (A) Complex C adsorbed on a cellulose nitrate filter reacted with (□) 4×10^{-6} M tylosin alone or with a solution containing 4×10^{-6} M tylosin and erythromycin at (■) 2×10^{-7} M, (●) 5×10^{-7} M, (▲) 1×10^{-6} M, (▼) 2×10^{-6} M, (◆) 3×10^{-6} M, (○) 5×10^{-6} M, and (△) 2×10^{-5} M. (B) Variation of $1/F$ as a function of the erythromycin concentration. The parameter F represents the apparent rate constant of complex C inactivation, and its values were estimated from the slope of the A plots.

Scheme 3

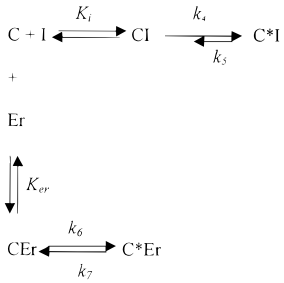

erythromycin is not equilibrated instantaneously, and this should be the isomerization step. By preincubating complex C with erythromycin to achieve steady state, not only the equilibrium C + Er ⇆ CEr but also the equilibrium CEr ⇄ C*Er is attained. Consequently, the value 3.6×10^{-8} M of the dissociation constant estimated under such conditions measures the overall dissociation constant (K_{er}*), which concerns both steps of erythromycin interaction with complex C, and is defined by the equation: $K_{er}^* = [C][Er]/([CEr] + [C^*Er])$. Once both K_{er} and K_{er}* have been estimated, the isomerization constant k_6/k_7 can be determined by the equation

$$K_{er}^* = K_{er}\left(\frac{k_7}{k_6 + k_7}\right) \qquad (5)$$

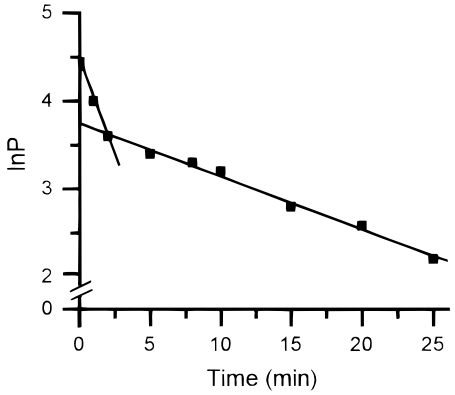

FIGURE 6: Determination of the dissociation rate constant, k_7, for the erythromycin complex C*Er. Complex C formed in the presence of 1×10^{-5} M erythromycin and adsorbed on a cellulose nitrate filter was exposed to 1×10^{-5} M tylosin for various time intervals, and then the remaining activity was titrated by 2 mM puromycin. The k_7 value was estimated from the late slope of the plot.

which is predicted by the slow-onset type of inhibition (*23*). The value of this ratio equals 10.

To calculate the individual values of k_6 and k_7, complex C preincubated with erythromycin and isolated on cellulose nitrate filters was exposed to tylosin at various time intervals, and the remaining activity was titrated with puromycin. The reaction displays two phases giving an early and a late slope (Figure 6). We suggest that the early slope represents the reaction of tylosin mostly with preexisting free complex C, while the late slope corresponds to the reaction of tylosin with complex C regenerated from the erythromycin complex C*Er via the k_7 step of the kinetic scheme. From the late slope, a value of k_7 equal to (0.060 ± 0.005) min^{-1} is calculated, independently of the tylosin concentration. The same value of k_7 was obtained when complex C*Er isolated on the cellulose nitrate filter was exposed to a large volume of buffer (100 mM Tris-HCl, pH 7.2/100 mM NH_4Cl/10 mM Mg^{2+} (acetate)/ 6 mM 2-mercaptoethanol) at 25 °C for specific time intervals, immersed in 3×10^{-5} M tylosin solution for 3 min, and then titrated with puromycin (2 mM, 2 min). With k_7 and k_6/k_7 known, the k_6 value is estimated as equal to 0.60 ± 0.05 min^{-1}.

Data Obtained from Experiments in Which the Reactions Take Place in Solution. To avoid artifacts from possible interface problems caused by the cellulose nitrate filters, the previous experiments were repeated using complex C desorbed in solution (*18*). The values of the kinetic parameters obtained are given in Table 1. For the sake of comparison, the values obtained with complex C adsorbed on a cellulose nitrate filter are also included.

DISCUSSION

Macrolides have been used extensively, not only for therapeutic purposes but also as tools for studying ribosome structure and function. Among them, tylosin and erythromycin have been frequently utilized (*27*). However, kinetic studies are scarce, and accidentally most of them have been carried out under the prevalent notion that the interaction between the ribosome (R) and the antibiotic (I) is expressed by a simple equilibrium of the form:

$$R + I \overset{K_i}{\rightleftharpoons} RI$$

Table 1: Kinetic and Equilibrium Constants Derived from Analysis of the Interaction between Complex C and the Macrolide Antibiotics Tylosin and Erythromycin[a]

	complex C on the filter		complex C in solution	
constant	tylosin	erythromycin	tylosin	erythromycin
K_i (μM)	3.00 ± 0.03		2.30 ± 0.02	
k_4 (min^{-1})	1.50 ± 0.04		1.80 ± 0.06	
k_5 ($min^{-1} \times 10^{-3}$)	2.50 ± 0.20		3.00 ± 0.20	
K_{er} (nM)		390 ± 16		40 ± 2
K_{er}* (nM)		36 ± 2		4.2 ± 0.2
k_6 (min^{-1})		0.60 ± 0.07		0.60 ± 0.06
k_7 (min^{-1})		0.060 ± 0.005		0.07 ± 0.005

[a] Data represent the mean ± SE values obtained from four, independently performed, experiments.

The present report postulates that the initial encounter complex between the ribosomal complex and the antibiotic is followed by a slowly equilibrated isomerization to a tight complex and that the use of constants additional to K_i is required to evaluate late events of the ribosome/drug interaction.

By monitoring the inhibition of the puromycin reaction by tylosin, as well as by direct measurement of peptidyltransferase inactivation by tylosin in the absence of puromycin, we established that tylosin derives its potency through a slow-binding inhibition mechanism. Tylosin interacts with complex C with an apparent association rate constant (k_4/K_i) of 0.8×10^4 M^{-1} s^{-1}. This value is much lower than the upper limit of 10^6 M^{-1} s^{-1} set for the characterization of a drug as a slow-binding inhibitor (*23*). However, slow-binding inhibition requires that the reverse isomerization rate constant (k_5) must be less than the forward isomerization rate constant (k_4). In the case of tylosin, this criterion is also satisfied, since the value of the k_4/k_5 ratio is equal to 600. This high value characterizes tylosin as a slow-binding, slowly reversible inhibitor of peptide bond formation and suggests that the C*I complex has a useful in vivo lifetime. Moreover, the low value of the k_5 rate constant gives us the opportunity to kinetically analyze the effect as if tylosin were an irreversible inhibitor. In the case of irreversible inhibitors, the type of inhibition can be revealed by studying the effect of substrate concentration on the apparent rate constant of inactivation (*28*). Such a method cannot be applied in our experimental system, since complex C is depleted during the reaction. Therefore, we followed another procedure of data elaboration, proposed for enzymes consumed in the reaction they catalyze (*24*). According to this analysis, the linearity of the C_0/AP_∞ versus 1/[S] plot suggests a competitive type of inhibition. Three mechanisms have been proposed to describe slow onset of competitive inhibition (*29*):

mechanism A

$$E + I \rightleftarrows EI$$

mechanism B

$$E + I \rightleftarrows EI \rightleftarrows E^*I$$

mechanism C

$$E \rightleftarrows E^* + I \rightleftarrows E^*I$$

To discriminate between the binding mechanisms, the relationships observed between A, P_∞/A, k_{in}, [S], and [I] were assessed. The observation that the apparent rate constant of inactivation A or k_{in} increases with increasing tylosin concentration (illustrated in Figure 1B and Figure 3A) is consistent with mechanism A and B but not with mechanism C. In the latter case, the inactivation rate constant should decline with increasing drug concentration. On the other hand, the initial slope of the semilogarithmic time plots (Figure 1A) significantly decreases in proportion with the inhibitor concentration, while the replot of A or k_{in} versus [I] is characterized by a hyperbolic shape, a finding inconsistent with mechanism A. To date, nearly all reported examples of slow-binding inhibition of the puromycin reaction by antibiotics exhibit biphasic inhibition pattern due to the formation of an initial CI complex followed by a unimolecular isomerization toward a more tight C*I complex (*30*, *31*). One exception reported earlier is the monophasic slow-binding inhibition of peptide bond formation by spiramycin, a 16-membered ring macrolide (*18*). Compared with spiramycin, tylosin shows a higher k_4/k_5 value, which is an index of C*I tightness, but exhibits a lower apparent association constant (k_4/K_i), which justifies the hypothesis that tylosin stabilizes, rather than induces, C*I formation. While most of the slow-binding inhibitors possess their kinetic properties by virtue of their structural similarity to transition state or intermediates of the enzymatic reactions inhibited (*23*, *32*), it is difficult to imagine which event in the peptide bond formation process might be resembled by tylosin or spiramycin. Other cases of slow-binding inhibitors, not behaving as transition-state or intermediate analogues, have been reported in the literature (*32*).

The tylosin reaction supplemented by the puromycin reaction can be used in the investigation of those antibiotics that fail to inhibit peptide bond formation. For instance, erythromycin does not inhibit AcPhe-puromycin formation, although it blocks the translation machinery (*5*). With the aid of the tylosin reaction we found that erythromycin interacts with complex C in a two-step mechanism, resembling the inhibition pattern exhibited by tylosin. The relatively low value of the apparent association constant ($k_6/K_{er} = 2.5 \times 10^4$ M^{-1} s^{-1}) and the fact that the reverse rate constant k_7 is less than the forward rate constant k_6 ($k_6/k_7 = 10$) allow us to characterize erythromycin as a slow-binding, slowly reversible drug, interacting with complex C. This finding confirms previous observations that the binding of erythromycin to bacterial ribosomes occurs in a two-step process: a first step involving a fast and weak interaction as revealed by TRNOE measurements (*9*) and a second step involving strong interaction, as measured by equilibrium dialysis (*33*), fluorescence kinetic analysis (*17*, *34*), and footprinting analysis (*16*). In the present work, the K_{er} value corresponding to the fast equilibrated step $C + I \rightleftarrows CI$ was found to be lower than that obtained by TRNOE analysis. We assume that the observed difference may be due to the fact that, instead of vacant ribosomes, complex C is used in our experimental system. Nevertheless, the calculated value of the overall dissociation constant ($K_{er}^* = 3.6 \times 10^{-8}$ M) is in close proximity to values reported previously (*16*, *17*, *33*, *34*). It should be mentioned that, although there are some differences in the values of the K_{er} and K_{er}* equilibrium constants (Table 1), the mechanism of tylosin or erythromycin interaction with complex C free in solution is similar to that observed with complex C adsorbed on a cellulose

nitrate filter. Consequently, it is evident that the slow-binding interaction between complex C and the examined antibiotics does not reflect interface artifacts.

Like other macrolides, the primary site of erythromycin interaction with ribosomes is at the central loop of domain V of 23S rRNA (*7*, *10*, and references therein). However, the footprinting pattern of erythromycin in this loop is distinctive from that caused by macrolides with a 16-membered ring. This may be the first reason why erythromycin does not inhibit the puromycin reaction, while the second one is probably due to the small molecular size of the drug, which does not permit functional groups of erythromycin to extend into the catalytic cavity of peptidyltransferase (*4*, *35*). In support of this hypothesis, it has been reported that puromycin, erythromycin, deacylated tRNA, and a peptidyl-tRNA analogue can be bound simultaneously to the same ribosome (*13*). Despite the inability of erythromycin to inhibit the puromycin reaction, this drug, upon binding to the ribosome, causes a conformational change in the local environment of the P-site and the entrance of nascent peptide (*10*, *13*). This effect could explain the rearrangement of the encounter complex CEr to another C*Er more tight species.

On the basis of the arguments developed for slow-onset inhibition of enzymes (*23*, *32*), the slow-onset association of tylosin and erythromycin with complex C acquires biological significance. From the standpoint of drug design for pharmaceutical applications, a slow rate of dissociation is desirable as it may be expected to result in a longer lived C*I complex, while a slow rate of association should be avoided since it delays the time required for inhibition at a given concentration. The present work postulates that whenever a drug interaction with ribosomes is investigated, an appropriate experimental system is required to reveal possible late events of interaction. In such cases, the full characterization of drug potency requires the use of constants additional to K_i.

ACKNOWLEDGMENT

We thank Dr. Dennis Synetos for critical reading of the manuscript.

APPENDIX

In Scheme 3, complex C is inactivated by tylosin. This inactivation is protected by erythromycin. In deriving the corresponding equations, it is assumed that the equilibria C + I $\leftrightarrows$ CI and C + Er $\rightleftarrows$ CEr are established rapidly, while the isomerizations CI $\rightleftarrows$ C*I and CEr $\rightleftarrows$ C*Er are established slowly. Under these assumptions, one can write

$$K_i = \frac{[C][I]}{[CI]} \quad \text{or} \quad [C] = \frac{K_i[CI]}{[I]} \tag{A1}$$

$$K_{er} = \frac{[C][Er]}{[CEr]} \quad \text{or} \quad [CEr] = \frac{[C][Er]}{K_{er}} = \frac{K_i[CI][Er]}{K_{er}[I]} \tag{A2}$$

Erythromycin does not inhibit the puromycin reaction. Consequently, both CEr and C*Er species react with puromycin, and the concentration of noninactivated complex C, $[C_T]$, is given by the equation:

$$[C_T] = [C] + [CI] + [CEr] + [C^*Er] \tag{A3}$$

As time approaches 0 and complex C reacts with a mixture of tylosin and erythromycin, the concentration of C*Er is negligible. Thus, eq A3 can also be written

$$[C_T] = \frac{K_i[CI]}{[I]} + [CI] + \frac{[Er]K_i[CI]}{K_{er}[I]} = [CI] \times \left[\frac{K_iK_{er} + K_{er}[I] + K_i[Er]}{K_{er}[I]}\right] \tag{A4}$$

The differential of C_T is given by the equation:

$$C_T = C_0 e^{-F\,t} \tag{A5}$$

where

$$F = \frac{k_4K_{er}[I]}{K_iK_{er} + K_{er}[I] + K_i[Er]} \tag{A6}$$

Equation A6 can be written also as

$$\frac{1}{F} = \frac{K_i + [I]}{k_4[I]} + \frac{K_i[Er]}{k_4K_{er}[I]} \tag{A7}$$

or

$$\frac{1}{F} = \frac{1}{k_4} + \frac{K_i\left(1 + \frac{[Er]}{K_{er}}\right)}{k_4}\frac{1}{[I]} \tag{A8}$$

C_T can be measured by titration with puromycin, which converts C_T to product P. If we substitute C_T in eq A5 with its equivalent P, we obtain

$$P = C_0 e^{-F\,t} \quad \text{or} \quad \ln\frac{C_0}{P} = Ft \tag{A9}$$

From the plot of $\ln[C_0/P]$ or $\ln P$ versus t, one can experimentally obtain the apparent rate constant F for the inactivation of complex C at each concentration of both I and Er. With K_i and k_4 known, the value of K_{er} can be estimated by plotting $1/F$ versus [Er] (see eq A7) or $1/F$ versus $1/[I]$ (see eq A8).

When preincubation of complex C with erythromycin precedes the addition of tylosin, the sequential reactions

$$C + Er \overset{K_{er}}{\rightleftharpoons} CEr \underset{k_7}{\overset{k_6}{\rightleftharpoons}} C^*Er$$

have reached a steady-state equilibrium. Under this assumption, eq A8 is transformed to the equation

$$\frac{1}{F} = \frac{1}{k_4} + \frac{K_i\left(1 + \frac{[Er]}{K_{er}^*}\right)}{k_4}\frac{1}{[I]} \tag{A10}$$

where $K_{er}^* = K_{er}[k_7/(k_6 + k_7)]$ (*23*). From eq A10, the value

of K_{er}* can be calculated in a manner similar to that followed for the estimation of the K_{er} value.

REFERENCES

1. Gale, E. F., Cundliffe, E., Reynolds, P. E., Richmond, M. H., and Waring, M. J. (1981) *The Molecular Basis of Antibiotic Action*, John Wiley & Sons, London.
2. Ballesta, J. P. G., and Lazaro, E. C. (1990) in *The Ribosome, Structure Function and Evolution* (Hill, W., Dahlberg, A., Garrett, R., Moore, P., Schlessinger, D., and Warner, J., Eds.) pp 502−510, AMS Press, Washington, DC.
3. Spahn, C. M. T., and Prescott, C. D. (1996) *J. Mol. Med. 74*, 423−439.
4. Porse, B. T., Rodriguez-Fonseca, C., Leviev, I., and Garrett, R. A. (1995) *Biochem. Cell Biol. 73*, 877−885.
5. Vazquez, D. (1979) *Mol. Biol. Biochem. Biophys. 30*, 1−312.
6. Moureau, P., Engelborghs, Y., Di Giambattista, M., and Cocito, C. (1983) *J. Biol. Chem. 258*, 14233−14238.
7. Moazed, D., and Noller, H. F. (1987) *Biochimie 69*, 879−884.
8. Di Giambattista, M., Nyssen, E., Pecher, A., and Cocito, C. (1990) *Biochemistry 29*, 9203−9211.
9. Bertho, G., Gharbi-Benarous, J., Delaforge, M., and Girault, J.-P. (1998) *Bioorg. Med. Chem. 6*, 209−221.
10. Hansen, L. H., Mauvais, P., and Douthwaite, S. (1999) *Mol. Microbiol. 31*, 623−631.
11. Menninger, J. R., and Otto, D. P. (1982) *Antimicrob. Agents Chemother. 21*, 811−818.
12. Chinali, G., Nyssen, E., Di Giambattista, M., and Cocito, C. (1988) *Biochim. Biophys. Acta 951*, 42−52.
13. Odom, O. W., Picking, W. D., Tsalkova, T., and Hardesty, B. (1991) *Eur. J. Biochem. 198*, 713−722.
14. Champney, W. S., and Burdine, R. (1996) *Antimicrob. Agents Chemother. 40*, 1301−1303.
15. Weisblum, B. (1995) *Antimicrob. Agents Chemother. 39*, 577−585.
16. Douthwaite, S., and Aagaard, C. (1993) *J. Mol. Biol. 232*, 725−731.
17. Di Giambattista, M., Engelborghs, Y., Nyssen, E., and Cocito, C. (1987) *J. Biol. Chem. 262*, 8591−8597.
18. Dinos, G. P., Synetos, D., and Coutsogeorgopoulos, C. (1993) *Biochemistry 32*, 10638−10647.
19. Kalpaxis, D. L., Theocharis, D. A., and Coutsogeorgopoulos, C. (1986) *Eur. J. Biochem. 154*, 267−271.
20. Theocharis, D. A., and Coutsogeorgopoulos, C. (1989) *Anal. Biochem. 176*, 278−283.
21. Daniel, W. W. (1988) *Biostatistics: A Foundation for Analysis in the Health Sciences*, John Wiley & Sons, New York.
22. Synetos, D., and Coutsogeorgopoulos, C. (1987) *Biochim. Biophys. Acta 923*, 275−285.
23. Morrison, J. F., and Walsh, C. T. (1988) *Adv. Enzymol. Relat. Areas Mol. Biol. 61*, 201−301.
24. Dinos, G. P., and Coutsogeorgopoulos, C. (1997) *J. Enzyme Inhibit. 12*, 79−99.
25. Kitz, R., and Wilson, I. B. (1962) *J. Biol. Chem. 237*, 3245−3249.
26. Erion, M. D., and Walsh, C. T. (1987) *Biochemistry 26*, 3417−3425.
27. Wilson, R. C. (1984) in *Macrolide Antibiotics, Chemistry, Biology and Practice* (Omura, S., Ed.) pp 301−347, Academic Press, New York.
28. Tian, W. X., and Tsou, C. L. (1982) *Biochemistry 21*, 1028−1032.
29. Cha, S. (1975) *Biochem. Pharmacol. 24*, 2177−2185.
30. Theocharis, D. A., Synetos, D., Kalpaxis, D. L., Drainas, D., and Coutsogeorgopoulos, C. (1992) *Arch. Biochem. Biophys. 292*, 266−272.
31. Kallia-Raftopoulos, S., Kalpaxis, D. L., and Coutsogeorgopoulos, C. (1992) *Arch. Biochem. Biophys. 298*, 332−339.
32. Schloss, J. V. (1988) *Acc. Chem. Res. 21*, 348−353.
33. Pestka, S. (1974) *Antimicrob. Agents Chemother. 6*, 474−478.
34. Langlois, R., Cantor, C. R., Vince, R., and Pestka, S. (1977) *Biochemistry 16*, 2349−2356.
35. Kirillov, S., Porse, B. T., Vester, B., Woolley, P., and Garrett, R. A. (1997) *FEBS Lett. 406*, 223−233.

BI000811F